identified another PTCL case positive for the R634H polymorphism. While the cohort size is still small, frequency (2/92=2.2%) of this polymorphism in PTCL is significantly over-represented compared to that (1/2385=0.04%) in the 1000 genome database ($P=4.0x10^{-3}$, Fisher's exact test).

Noteworthy, some of the somatic mutations within STK10 found in epithelial tumors have more profound effects on the NF-κB regulation and cell apoptosis than R634H. Thus, dysfunction of STK10 through somatic mutations is likely a novel, driver event in human carcinogenesis. Restoration of STK10 function or/and suppression of NF-κB in the tumors positive for STK10 mutations can be a novel strategy for raising effective molecular targeted therapies against human cancer.

Acknowledgements

This study was supported in part by grants for Third-Term Comprehensive Control Research for Cancer and for Research on Human Genome Tailor-made from the Ministry of Health, Labor and Welfare of Japan, by Grants-in-Aid from the Japan Society for the Promotion of Science, from The Yasuda Medical Foundation, from The Sagawa Foundation for Promotion of Cancer Research, and from The Mitsubishi Foundation.

References

1. Lynch TJ, Bell DW, Sordella R, *et al*: Activating mutations in the epidermal growth factor receptor underlying responsiveness of non-small-cell lung cancer to gefitinib. N Engl J Med 350: 2129-2139, 2004.
2. Soda M, Choi YL, Enomoto M, *et al*: Identification of the transforming *EML4-ALK* fusion gene in non-small-cell lung cancer. Nature 448: 561-566, 2007.
3. Mok TS, Wu YL, Thongprasert S, *et al*: Gefitinib or carboplatin-paclitaxel in pulmonary adenocarcinoma. N Engl J Med 361: 947-957, 2009.
4. Kwak EL, Bang YJ, Camidge DR, *et al*: Anaplastic lymphoma kinase inhibition in non-small-cell lung cancer. N Engl J Med 363: 1693-1703, 2010.
5. Foss FM, Zinzani PL, Vose JM, Gascoyne RD, Rosen ST and Tobinai K: Peripheral T-cell lymphoma. Blood 117: 6756-6767, 2011.
6. Vose J, Armitage J and Weisenburger D: International peripheral T-cell and natural killer/T-cell lymphoma study: pathology findings and clinical outcomes. J Clin Oncol 26: 4124-4130, 2008.
7. Gambacorti-Passerini C, Messa C and Pogliani EM: Crizotinib in anaplastic large-cell lymphoma. N Engl J Med 364: 775-776, 2011.
8. Ueno T, Yamashita Y, Soda M, *et al*: High-throughput resequencing of target-captured cDNA in cancer cells. Cancer Sci 103: 131-135, 2012.
9. Hu Q, Milfay D and Williams LT: Binding of NCK to SOS and activation of ras-dependent gene expression. Mol Cell Biol 15: 1169-1174, 1995.
10. Takeshita T, Arita T, Higuchi M, *et al*: STAM, signal transducing adaptor molecule, is associated with Janus kinase and involved in signaling for cell growth and c-myc induction. Immunity 6: 449-457, 1997.
11. Grillot DAM, Gonzalez-Garcia M, Ekhterae D, *et al*: Genomic organization, promoter region analysis, and chromosome localization of the mouse *bcl-x* gene. J Immunol 158: 4750-4757, 1997.
12. Kurooka H, Kuroda K and Honjo T: Roles of the ankyrin repeats and C-terminal region of the mouse notch1 intracellular region. Nucleic Acids Res 26: 5448-5455, 1998.
13. Hill CS, Wynne J and Treisman R: The Rho family GTPases RhoA, Rac1, and CDC42Hs regulate transcriptional activation by SRF. Cell 81: 1159-1170, 1995.
14. Walter SA, Cutler RE Jr, Martinez R, Gishizky M and Hill RJ: Stk10, a new member of the polo-like kinase kinase family highly expressed in hematopoietic tissue. J Biol Chem 278: 18221-18228, 2003.
15. Jost PJ and Ruland J: Aberrant NF-kappaB signaling in lymphoma: mechanisms, consequences, and therapeutic implications. Blood 109: 2700-2707, 2007.
16. Choi YL, Soda M, Ueno T, *et al*: Oncogenic MAP2K1 mutations in human epithelial tumors. Carcinogenesis 33: 956-961, 2012.
17. Dan I, Watanabe NM and Kusumi A: The Ste20 group kinases as regulators of MAP kinase cascades. Trends Cell Biol 11: 220-230, 2001.
18. Kuramochi S, Moriguchi T, Kuida K, Endo J, Semba K, Nishida E and Karasuyama H: LOK is a novel mouse STE20-like protein kinase that is expressed predominantly in lymphocytes. J Biol Chem 272: 22679-22684, 1997.

Cancer Science
The official journal of the Japanese Cancer Association JCA

Cancer-associated missense mutations of caspase-8 activate nuclear factor-κB signaling

Mizuo Ando,[1,2] Masahito Kawazu,[1] Toshihide Ueno,[3] Kazutaka Fukumura,[1] Azusa Yamato,[3] Manabu Soda,[3] Yoshihiro Yamashita,[3] Young L. Choi,[1] Tatsuya Yamasoba[2] and Hiroyuki Mano[1,3,4,5,6]

Departments of [1]Medical Genomics; [2]Otolaryngology and Head and Neck Surgery, Graduate School of Medicine, University of Tokyo, Tokyo; [3]Division of Functional Genomics, Jichi Medical University, Tochigi; [4]Department of Cellular Signaling, Graduate School of Medicine, University of Tokyo, Tokyo; [5]CREST, Japan Science and Technology Agency, Saitama, Japan

(Received December 7, 2012/Revised April 26, 2013/Accepted May 6, 2013/Accepted manuscript online May 9, 2013/Article first published online June 7, 2013)

Head and neck squamous cell carcinoma (HNSCC) is an aggressive cancer with a 5-year survival rate of ~50%. With the use of a custom cDNA-capture system coupled with massively parallel sequencing, we have now investigated transforming mechanisms for this malignancy. The cDNAs of cancer-related genes (n = 906) were purified from a human HNSCC cell line (T3M-1 Cl-10) and subjected to high-throughput resequencing, and the clinical relevance of non-synonymous mutations thus identified was evaluated with luciferase-based reporter assays. A CASP8 (procaspase-8) cDNA with a novel G-to-C point mutation that results in the substitution of alanine for glycine at codon 325 was identified, and the mutant protein, CASP8 (G325A), was found to activate nuclear factor-κB (NF-κB) signaling to an extent far greater than that achieved with the wild-type protein. Moreover, forced expression of wild-type CASP8 suppressed the growth of T3M-1 Cl-10 cells without notable effects on apoptosis. We further found that most CASP8 mutations previously detected in various epithelial tumors also increase the ability of the protein to activate NF-κB signaling. Such NF-κB activation was shown to be mediated through the COOH-terminal region of the second death effector domain of CASP8. Although CASP8 mutations associated with cancer have been thought to promote tumorigenesis as a result of attenuation of the proapoptotic function of the protein, our results now show that most such mutations, including the novel G325A identified here, separately confer a gain of function with regard to activation of NF-κB signaling, indicating another role of CASP8 in the transformation of human malignancies including HNSCC. (*Cancer Sci* 2013; 104: 1002–1008)

Head and neck squamous cell carcinoma (HNSCC) is one of the most common types of human cancer, with an annual incidence of more than 500 000 cases worldwide.[1,2] The major risk factors for HNSCC are tobacco use, alcohol consumption, and infection with human papilloma virus.[3] It is an aggressive cancer with a propensity for local invasion and metastasis, which directly leads to disease- or treatment-related morbidity. The goals of HNSCC treatment are therefore not only to improve survival outcome but also to preserve vital physiological functions such as speech, breathing, swallowing, and hearing.

Most patients with HNSCC, however, present with advanced disease at the time of first evaluation and have a 5-year survival rate of only ~50%. Although advances in surgery and chemoradiation treatment have helped to preserve organ function in such individuals, they have resulted in only a moderate improvement in patient survival during the past 30 years. Characterization of the molecular mechanisms of HNSCC oncogenesis is expected to provide important information for the development of novel anticancer agents and the identification of biomarkers.

The recent advent of massively parallel sequencers, or next-generation sequencers, has rendered resequencing of the cancer genome manageable in private laboratories.[4] We have recently shown that a custom cDNA-capture system coupled with massively parallel sequencing provides a feasible and relatively simple approach for the simultaneous detection of point mutations, insertions/deletions (indels), and gene fusions among the captured genes.[5] Here we show that such high-throughput resequencing of targeted cDNAs from an oral squamous cell carcinoma cell line led to the identification of a missense mutation in caspase-8 (CASP8), a member of the cysteine–aspartic acid protease (caspase) family. Unexpectedly, CASP8 with this amino acid substitution (glycine-325 to alanine, or G325A) was found to activate signaling by the antiapoptotic transcription factor nuclear factor-κB (NF-κB) to an extent markedly greater than that observed with the wild-type protein. Of interest, most CASP8 mutants previously identified in human cancers were also found to activate the NF-κB pathway. As far as we are aware, a direct antiapoptotic effect of CASP8 in cancer has not previously been demonstrated.

Materials and Methods

Cell lines and plasmids. Human embryonic kidney 293T (HEK293T) cells, human oral squamous cell carcinoma T3M-1 Cl-10 cells, and human esophageal squamous cell carcinoma OE21 cells were obtained from RIKEN Cell Bank (Tsukuba, Japan), ATCC (Manassas, VA, USA), and European Collection of Cell Cultures (Salisbury, UK), respectively. All cells were maintained in DMEM–F12 supplemented with 10% FBS and 2 mM L-glutamine (all of which were from Invitrogen, Carlsbad, CA, USA). A full-length cDNA for the G325A mutant form of CASP8 was isolated by RT-PCR from T3M-1 Cl-10 cells and inserted into the retroviral plasmid pMXS.[6] Expression vectors for wild-type and previously identified mutant forms of CASP8 were generated by PCR-based mutagenesis. The nucleotide sequences of all constructs were confirmed by Sanger sequencing.

Resequencing coupled with a cDNA-capture system. Resequencing coupled with a custom cDNA-capture system was carried out as described previously.[5] In brief, RNA capture probes (Agilent Technologies, Santa Clara, CA, USA) designed to cover cDNAs of 906 human protein-coding genes were hybridized with cDNA fragments prepared from T3M-1 Cl-10 cells according to the protocols for the SureSelect Target Enrichment system (Agilent Technologies). Purified cDNA fragments were then subjected to deep sequencing for 76 bases from both ends with a Genome Analyzer IIx (GAIIx; Illumina, San Diego, CA, USA). Reads with a Q-value ≥20 at every

[6]To whom correspondence should be addressed.
E-mail: hmano@m.u-tokyo.ac.jp

doi: 10.1111/cas.12191
© 2013 Japanese Cancer Association

base were selected, and mapped to the reference cDNA sequences as well as the human genome sequence (GRCh37) with the Bowtie algorithm.[7] After removing single nucleotide polymorphisms (dbSNP build 32; http://www.ncbi.nlm.nih.gov/projects/SNP/snp_summary.cgi), non-synonymous mutations (≥30% mutation ratio at ≥30× coverage) for the target cDNAs were isolated by our in-house pipeline.

Luciferase-based reporter assays. The HEK293T cells were transfected with a CASP8 expression vector, the pGL-TK plasmid (Promega, Madison, WI, USA), and a luciferase-based reporter plasmid for signaling by c-Fos (pFL700),[8] c-Myc (pHXL),[9] β-catenin (TOP-flash; Upstate Biotechnology, Lake Placid, NY, USA), JNK (AP1; Panomics, Santa Clara, CA, USA), TP53,[10] Notch (pGa981-6),[11] Rho (pSRE.L),[12] MAPK (ELK1; Panomics), Gli (Genentech, South San Francisco, CA, USA), or NF-κB (Agilent Technologies). Luciferase activities were then assayed with a Dual-Luciferase Reporter Assay System (Promega), and the activity of firefly luciferase was normalized by that of *Renilla* luciferase.

Apoptosis and cell proliferation assays. The T3M-1 Cl-10 cells, which express CASP8(G325A), and OE21 cells, which express wild-type CASP8, were infected with a retrovirus generated from the pMXS-CASP8-ires-EGFP vector (Clontech, Mountain View, CA, USA), which allows simultaneous expression of CASP8 and enhanced green fluorescent protein (EGFP). The cells were then collected and assayed for apoptosis by staining with annexin V and propidium iodide (eBioscience, San Diego, CA, USA) followed by flow cytometry (FACSCanto II instrument; BD Biosciences, San Jose, CA, USA). Cell apoptosis was quantified by the Click-iT TUNEL Alexa Fluor Imaging Assay (Invitrogen). Cell proliferation was assayed by flow cytometric determination of the cell fraction positive for EGFP.

Statistical analysis. Quantitative data are presented as means ± SD and were compared with Student's *t*-test. A *P*-value of <0.05 was considered statistically significant.

Results

Identification of a CASP8 mutation in T3M-1 Cl-10 cells. To identify oncogenes for oral squamous cell carcinoma, we selected cDNA fragments for cancer-related genes (n = 906) from T3M-1 Cl-10 oral squamous cell carcinoma cells with the use of our custom cDNA-capture system.[5] Deep sequencing of such fragments with a GAIIx sequencer yielded 91 961 299 independent high-quality reads that mapped to 850 cDNAs with a mean coverage of 1202 reads/bp. Screening for missense mutations, indels, and gene fusions with our in-house computational pipeline resulted in the identification of 12 non-synonymous mutations that were further confirmed by Sanger sequencing (Table 1). We did not detect any indels or gene fusions that were confirmed by the capillary sequencing.

The 12 missense mutations include a novel G-to-C change at position 1183 of *CASP8* cDNA (GenBank accession number, NM_033355.3), which results in a glycine-to-alanine substitution at codon 325 of the encoded protein (Fig. 1a), as well as known HNSCC-related mutations such as those in *TP53* and *HRAS*. In our deep sequencing data, this substituted position of *CASP8* cDNA was read at a depth of ×469 and showed a mutation ratio of 98.5%, indicative of loss of heterozygosity at this locus.

The *CASP8* gene encodes the inactive (pro) form of CASP8, which plays an essential role in the execution of apoptosis.[13] Caspase-8 is composed of a COOH-terminal catalytic domain and an NH_2-terminal prodomain region that contains two tandem death effector domains (DEDs) (Fig. S1). Activation of CASP8 requires autoproteolysis that generates a heterodimer consisting of large (p20) and small (p10) protease subunits. The G325A mutation of CASP8 is located near the catalytic site in the p20 subunit.

Mutant CASP8(G325A) activates the NF-κB signaling pathway. To evaluate the biological relevance of the CASP8 (G325A) mutant, we carried out a reporter assay for a wide range of intracellular signaling pathways. Wild-type CASP8 markedly increased reporter activity for the NF-κB pathway (Fig. 1b), consistent with previous observations.[14,15] The G325A mutant of CASP8, however, increased such reporter activity to an extent far greater than that observed with the wild-type protein. In contrast, the effects of the wild-type and mutant forms of CASP8 on other signaling pathways, including those mediated by c-Fos, c-Myc, β-catenin, JNK, TP53, Notch, Rho, MAPK, and Gli, did not differ significantly (Fig. 1c), indicating that the G325A mutation influences NF-κB signaling specifically.

Catalytic activity of CASP8 and its mutants was also examined. The wild-type CASP8, CASP8(G325A), CASP8(C360A) (an amino acid substitution at the catalytic center),[16] CASP8 (D210A/D216A) (double mutations at the autoprocessing region), or CASP8(D210A/D216A/D223A) (triple mutations at the autoprocessing region), was introduced into HEK293 cells that were then subjected to an enzymatic assay for CASP8. As expected, wild-type CASP8 is catalytically active in HEK293, but a mutation at its catalytic center almost abolished its processing potency (Fig. 2a). Interestingly, the G325A substitution severely hampered CASP8 activity. In contrast, CASP8 with mutations at the autoprocessing region carry a decreased, but apparent, processing ability.

To examine whether the G350A mutation contributes directly to malignant transformation, we infected T3M-1 Cl-10 cells harboring the mutant *CASP8* gene with a retrovirus encoding both EGFP and either wild-type CASP8 or the

Table 1. Non-synonymous mutations detected in T3M-1 Cl-10 cells

Gene	GenBank accession no.	Read coverage	Mismatch reads (%)	Nucleotide change	Amino acid change
CASP8	NM_033355	×469	98.5	1183G>C	G325A
ELF4	NM_001421	×188	39.8	1016C>A	L211M
GSG2	NM_031965	×119	100.0	1238T>C	V402A
HRAS	NM_005343	×613	25.1	370A>T	Q61L
IRAK2	NM_001570	×155	49.0	591C>T	S172L
NUAK2	NM_030952	×162	51.2	1427G>A	A434T
PDPK1	NM_002613	×226	37.6	1663G>C	E507Q
PRKCZ	NM_002744	×61	49.1	306C>T	R49C
PXK	NM_017771	×82	57.3	364A>G	I89V
RHOA	NM_001664	×1127	52.9	394G>C	E40Q
TP53	NM_000546	×234	97.8	1035A>G	R280G
TTBK2	NM_173500	×100	51.0	1402G>C	L321F

© 2013 Japanese Cancer Association

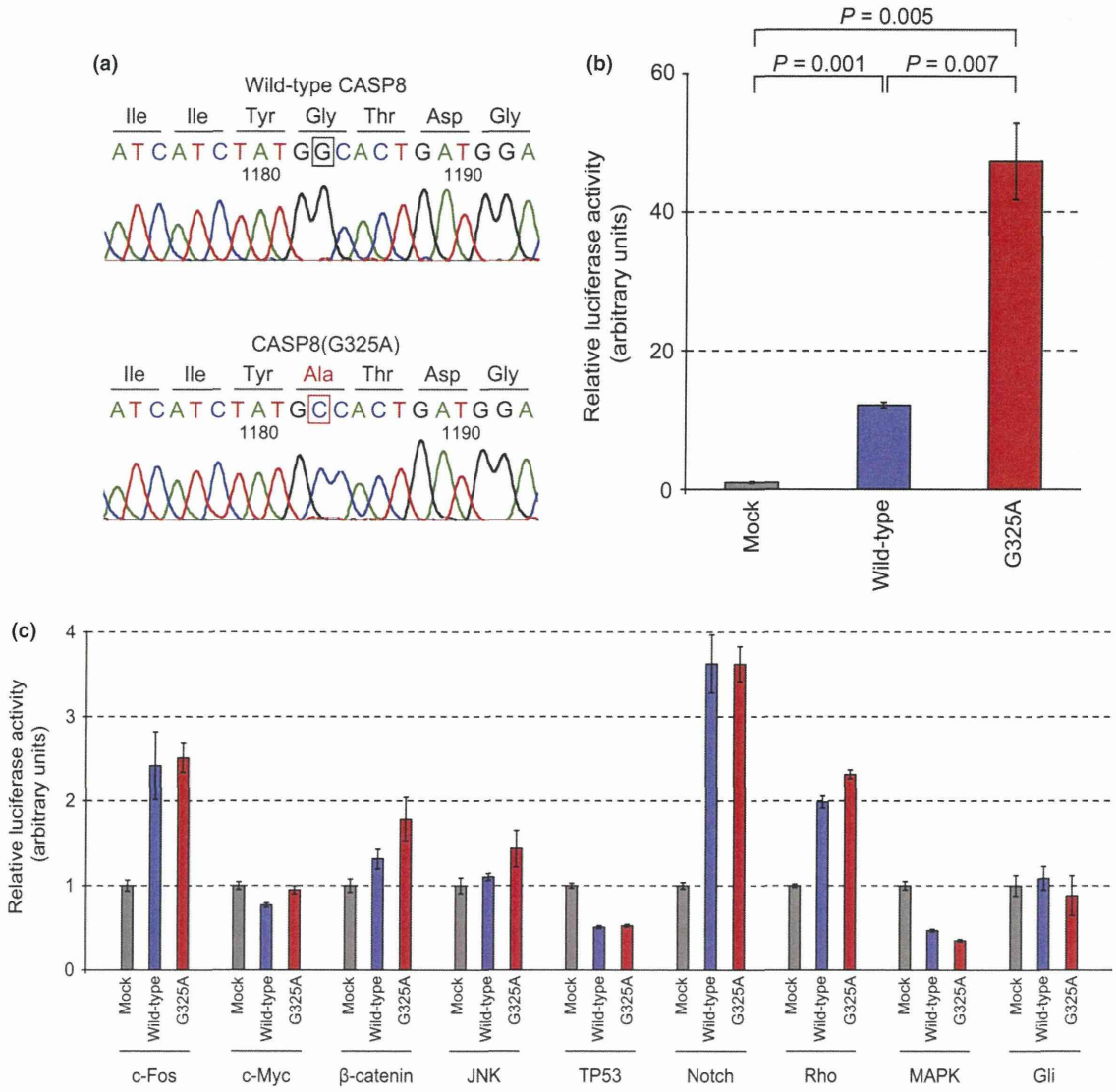

Fig. 1. Mutant protein CASP8(G325A) selectively activates the nuclear factor-κB (NF-κB) signaling pathway. (a) Electrophoretograms of *CASP8* cDNA identified an 1183G > C substitution, which results in a G325A amino acid substitution, in T3M-1 Cl-10 cells. (b,c) HEK293T cells were transfected with an expression vector for CASP8 or CASP8(G325A) or with the corresponding empty vector (Mock) together with pGL-TK and reporter plasmids for NF-κB (b) or other (c) signaling pathways, after which the cells were lysed and assayed for luciferase activities. The activity of firefly luciferase was normalized by that of *Renilla* luciferase then expressed relative to the corresponding value for mock-transfected cells. Data are means ± SD from three independent experiments. *P*-values were calculated using Student's *t*-test.

G325A mutant, then assayed the proliferation of EGFP-positive cells. Surprisingly, forced expression of wild-type CASP8 resulted in a marked reduction in the number of EGFP-positive cells, whereas the G325A mutant had only a slight effect on cell number (Fig. 2b). This suppression of cell growth by wild-type CASP8 was not observed in another squamous cell carcinoma cell line, OE21, which harbors the wild-type *CASP8* gene (Fig. 2b).

Interestingly, while annexin V-positive fraction was marginally increased in T3M-1 Cl-10 cells overexpressing wild-type CASP8 (Fig. S2), neither CASP8 nor CASP8 (G325A) induced notable apoptosis in T3M-1 Cl-10, as judged by the TUNEL assay (Fig. 2c). It is, therefore, possible that CASP8 regulation of cell growth in cancer may be independent, in part, of its apoptosis-inducing function.

We further depleted the *CASP8* message in T3M-1 Cl-10 by the use of siRNA, and examined its effects on the expression of NF-κB targets. As shown in Figure S3, decrease in the *CASP8* message led to a marked suppression in *BCL2* expression, supporting the positive role of CAPS8 in NF-κB signaling.

CASP8 mutations in human tumors. Non-synonymous mutations in CASP8 have been previously reported in various epithelial tumor types including gastric cancer (GC), colorectal cancer, hepatocellular carcinoma, and HNSCC.[16–19] These mutations include seven missense, one nonsense, and six frameshift mutations as well as one in-frame deletion (Fig. S1, Table S1). Whereas such mutations have been thought to contribute to carcinogenesis through a loss of the proapoptotic function of CASP8, we unexpectedly found that most of the mutants markedly activated NF-κB signaling (Fig. 3), suggestive of a gain of function with regard to such signaling. Of note, all of the three CASP8 mutants (GC1, GC4, and GC7) that failed to activate NF-κB signaling harbor non-synonymous mutations within the DEDs, suggesting that these domains may be essential for NF-κB activation.

In addition, screening as of January 2013 for non-synonymous mutations in CASP8 among public databases for

doi: 10.1111/cas.12191
© 2013 Japanese Cancer Association

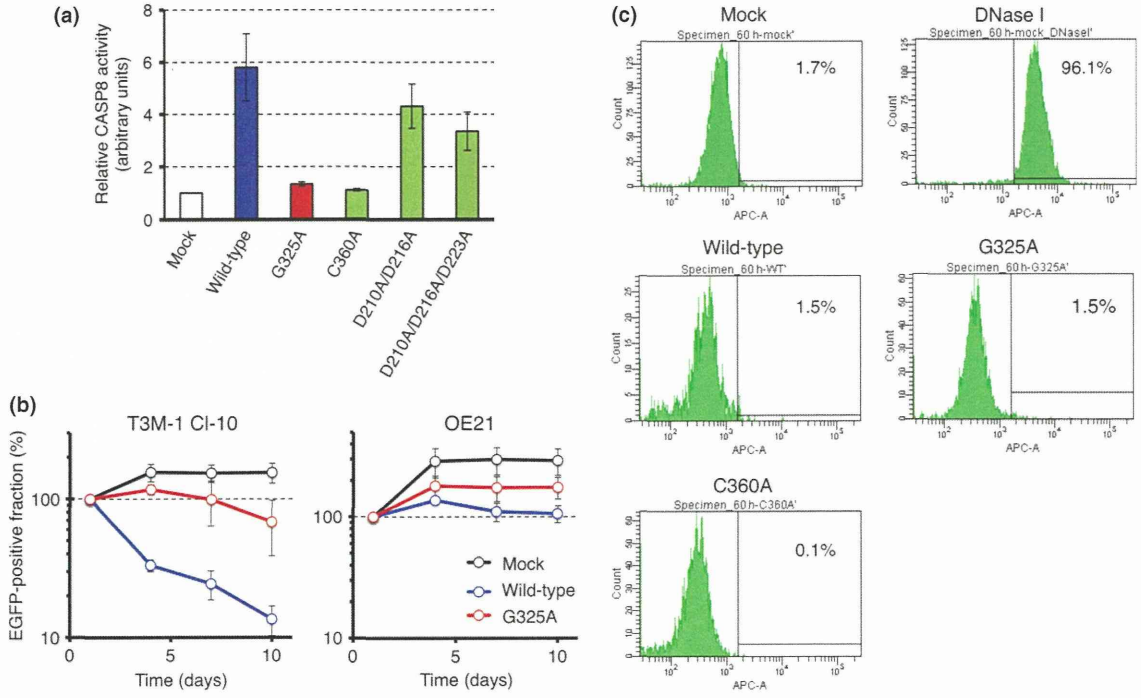

Fig. 2. Caspase-8 (CASP8) suppresses the proliferation of T3M-1 Cl-10 cells but not that of OE21 cells. (a) Proteolytic activity of CASP8 was measured with the Caspase-Glo8 assay for HEK293 cells expressing wild-type CASP8, CASP8(G325A), CASP8(C360A), CASP8(D210A/D216A), or CASP8(D210A/D216A/D223A), and is shown relative to the value for mock-transfected cells. Data are means ± SD from three independent experiments. (b) T3M-1 Cl-10 cells (left panel) or OE21 cells (right panel) were infected with a retrovirus encoding enhanced green fluorescent protein (EGFP) either alone (Mock) or together with wild-type or G325A mutant forms of CASP8. The number of EGFP-positive cells was then measured by flow cytometry at 1, 4, 7, and 10 days after infection and is expressed as a percentage of that at 1 day after infection. Data are means ± SD from three independent experiments. (c) Fragmented DNA in apoptotic cells was quantified by TUNEL assay for T3M-1 Cl-10 cells infected with an empty virus (Mock), or virus expressing wild-type, G325A mutant, or C360A mutant of CASP8. Fractions of cells with fragmented DNA are indicated as percentages. T3M-1 Cl-10 cells treated with DNase I were used as a positive control of apoptosis.

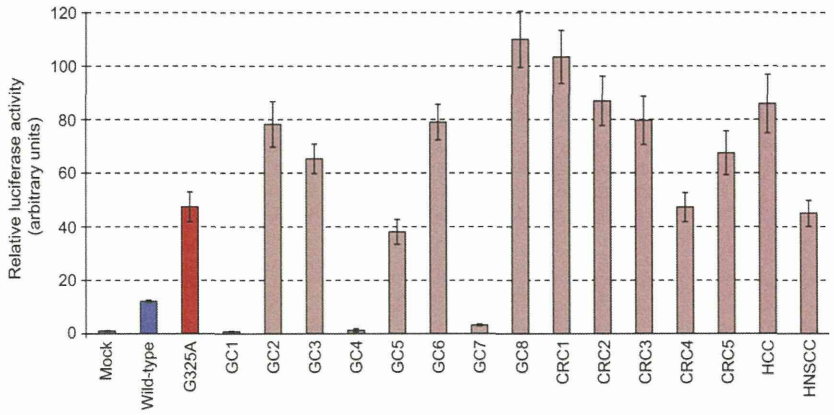

Fig. 3. Tumor-associated caspase-8 (CASP8) mutants activate the nuclear factor-κB pathway. HEK293T cells were transfected with a luciferase reporter plasmid for nuclear factor-κB, with pGL-TK, and with expression vectors for wild-type or the indicated mutant forms of CASP8. Normalized firefly luciferase activity was then determined and expressed relative to the value for mock-transfected cells. Data are means ± SD from three independent experiments. CRC, colorectal cancer; GC, gastric cancer; HCC, hepatocellular carcinoma; HNSCC, head and neck squamous cell carcinoma.

cancer genome mutations (COSMIC version 62, http://cancer.sanger.ac.uk/cancergenome/projects/cosmic/; The Cancer Genome Atlas, https://tcga-data.nci.nih.gov/tcga/tcgaHome2.jsp; and the International Cancer Genome Consortium, http://icgc.org) list 76 independent missense/nonsense mutations, seven frame-shift indels within CASP8, many of which had been confirmed to be somatic changes. Interestingly, amino acid substitutions at Gly-325 (including G325A) were identified in multiple cancer specimens (such as those for large intestine carcinoma and cervical squamous cell carcinoma), suggesting that missense mutations at this position are recurrent.

Caspase-8 domains linked to NF-κB activation. To investigate further how CASP8 controls the NF-κB pathway, we generated a series of CASP8 mutants (Fig. 4a). As shown in Figure 4(b), the D210A/D216A mutant is still able to activate NF-κB signaling by an extent similar to that achieved with the wild-type protein. Similarly, the addition of both D210A and D216A

© 2013 Japanese Cancer Association

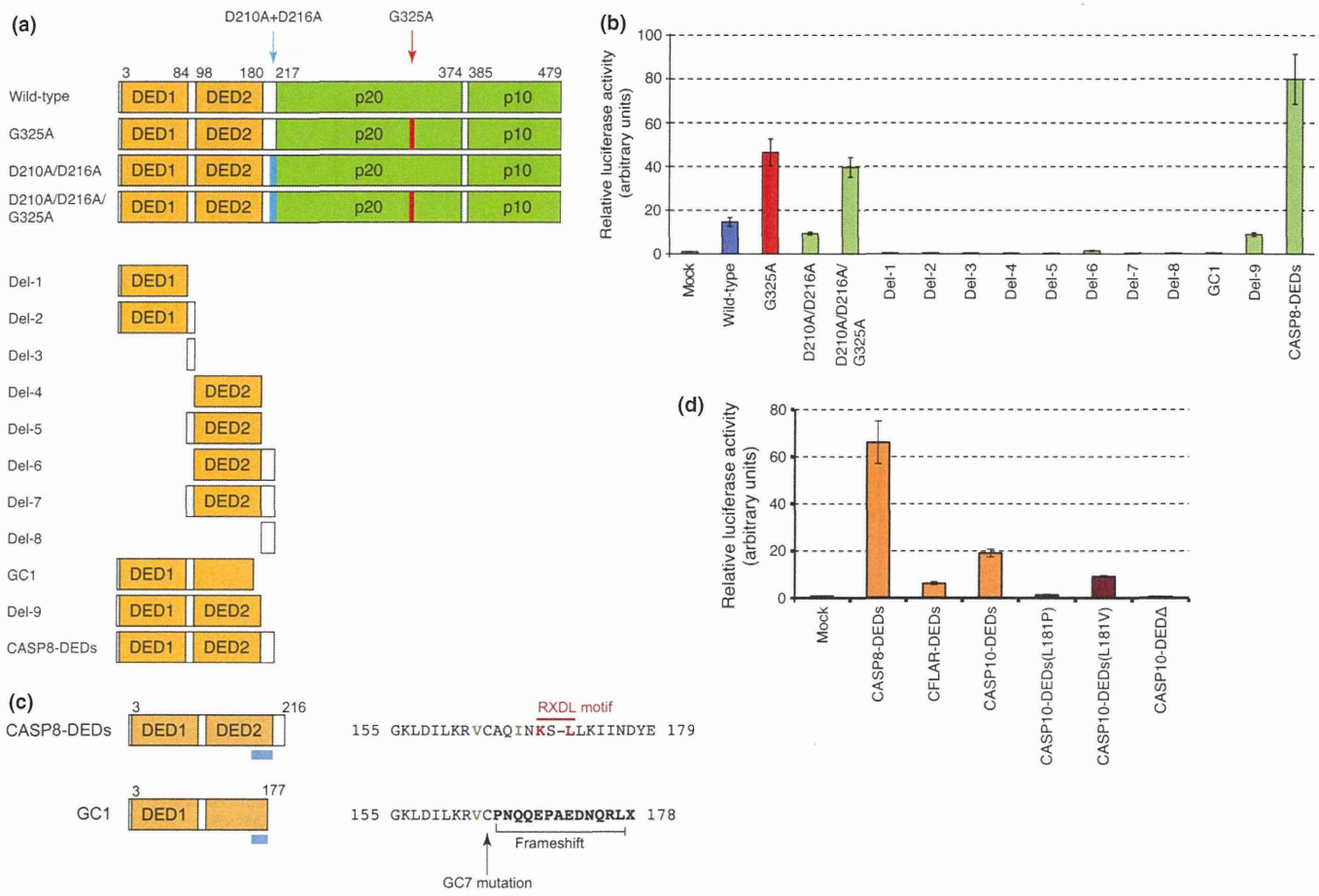

Fig. 4. Death effector domains (DEDs) activate nuclear factor-κB (NF-κB) signaling. (a) The protein structure of caspase-8 (CASP8) mutants is shown schematically with amino acid numbers indicated at the top. In addition to the wild-type and D210A/D216A mutant forms with or without the G325A substitution, various constructs for the DED and Hinge regions (Del-1 to Del-9) were generated. The structure of the mutant from cancer specimen GC1 and a mutant encompassing both DEDs and Hinge regions (CASP8-DEDs) is also shown. (b) Expression plasmids for the CASP8 mutants in (A) were introduced into HEK293T cells for the NF-κB reporter assay. Normalized firefly luciferase activity is expressed relative to the value for mock-transfected cells. Data are means ± SD from three independent experiments. (c) Amino acid sequences of the COOH-terminal regions (depicted by light blue bars in the left panel) of CASP8-DEDs and the CASP8 mutant from specimen GC1 are shown at the right. The conserved RXDL motif is indicated in red, and Val^{163} and Ile^{167} residues that contribute to the conserved hydrophobic patch are indicated in green. In the GC1 mutant, a frameshift deletion changes the amino acid sequence after Cys^{164} and generates a termination codon. The GC7 mutant has a C164Y substitution that markedly attenuates CASP8-induced NF-κB activation. (d) The ability to activate the NF-κB pathway was examined for CASP8-DEDs and the corresponding regions of CFLAR (amino acid residues 1–196) and CASP10 (residues 1–219), as in (b). For CASP10, we also examined the DED region with a L181P or L181V substitution, or RXDL-deleted DEDΔ encompassing only amino acid residues 1–175.

substitutions to CASP8(G325A) did not substantially affect its ability to activate the NF-κB pathway.

We also generated expression constructs for the NH_2-terminal DED (DED1) or COOH-terminal DED (DED2) either alone or together with the Hinge regions between DED1 and DED2 (Hinge-1) or between DED2 and p20 (Hinge-2) (Fig. 4a). None of these deletion mutants activated the NF-κB pathway (Fig. 4b). In contrast, a deletion mutant consisting of the entire prodomain (CASP8-DEDs) activated NF-κB signaling to a level even higher than that induced by CASP8 (G325A). Deletion of Hinge-2 from CASP8-DEDs (the Del-9 mutant) markedly reduced the stimulatory effect on NF-κB signaling. A *CASP8* cDNA previously identified in the specimen designated GC1 has a 2-bp deletion (Table S1) that results in premature termination within DED2 (Fig. 4c). This truncation almost completely abrogated the ability of CASP8 to activate NF-κB signaling (Figs 3,4b). Both Hinge-2 and the COOH-terminal end of DED2 thus likely play an essential role in the regulation of NF-κB signaling by CASP8. This notion was reinforced by the observation that a Cys^{164}-to-Tyr substitution at the COOH-terminal end of DED2 previously identified in the GC7 specimen (Table S1, Fig. 4c) also largely abolished the ability of CASP8 to activate NF-κB signaling (Fig. 3).

Members of the DED family of proteins possess a key hydrophobic patch (for DED–DED interactions) that is exposed at the surface of each molecule and includes the conserved RXDL motif (corresponding to "KS – L" in DED2 of CASP8) in the COOH-terminal region of the DED.[20–22] Our findings are thus consistent with the idea that this conserved region contributes to the regulation of NF-κB.

Prodomains of CASP8-related proteins are able to activate NF-κB signaling. Given that the prodomain of CASP8 is sufficient to fully active NF-κB signaling, we tested whether the prodomains of the CASP8-related proteins CFLAR (also known as cFLIPL) and caspase-10 (CASP10) might have similar effects. CFLAR is structurally similar to CASP8 but does not possess functional caspase activity, given that it does not

doi: 10.1111/cas.12191
© 2013 Japanese Cancer Association

contain the conserved catalytic cysteine residue found in all functional caspases.[23] Caspase-10 is highly homologous to CASP8 and is also recruited to, and becomes activated by, death receptors.[24–26] We found that the entire prodomains of CFLAR and CASP10 each markedly increased the level of NF-κB signaling (Fig. 4d) as already shown for CASP10 by other groups.[27] Although conservation of the RXDL motif is less clear in CASP10 compared to the other members (Fig. S4), substitution of the conserved Leu^{181} in CASP10 to either Pro or Val residues attenuated its NF-κB-activating potential (Fig. 4d). Furthermore, the CASP10-DEDs protein lacking the putative RXDL region completely lost such ability, confirming the essential role of the DEDs COOH-terminus in CASP10 activation of the NF-κB pathway.

Discussion

One of the most proximal caspases in the apoptosis cascade, CASP8 is driven by the death-inducing signaling complex in response to ligation of death receptors[13] such as tumor necrosis factor receptor 1, CD95 (Fas, or Apo1), and tumor necrosis factor-related apoptosis-inducing ligand (TRAIL, or Apo2L) receptor. Activation of CASP8 requires dimerization and consequent autocleavage of the procaspase-8 zymogen,[28] and it initiates the extrinsic apoptosis cascade through activation of downstream effectors such as CASP3, CASP6, and CASP7.[29]

In addition, CASP8 has the potential to activate the antiapoptotic transcription factor NF-κB through its tandem DED region,[14,15,30] and IκB kinase γ (IKKγ), an essential regulatory subunit of the IKK complex, participates in this CASP8-mediated activation of NF-κB.[31] The tandem DEDs of CFLAR also directly interact with and recruit IKKγ and thereby activate NF-κB.[32] However, we failed to detect a direct association between the tandem DEDs of CASP8 and IKKγ (data not shown). How the tandem DEDs of CASP8 mediate NF-κB activation thus remains unclear. Given the essential role of the COOH-terminal region of DED2 and the Hinge-2 region of CASP8 in the activation of NF-κB, it will be of interest to profile the cellular proteins that associate with these regions. Importantly, whereas somatic non-synonymous mutations in *CASP8* are detected relatively frequently in human tumors, the mutant proteins have been assumed to accelerate carcinogenesis as a result of a loss of proapoptotic function.[16,18,19]

In contrast, our data now suggest that many of the somatic mutations within *CASP8* in human cancer provide simultaneously inactivation of its proapoptotic function and activation of NF-κB signaling. Additionally, restoration of *CASP8* expression in a *CASP8*-mutant cell line (T3M-1 Cl-10) clearly suppressed cell proliferation without apparent effects on apoptosis, further confirming the relevance of *CASP8* mutation on carcinogenesis. It should be noted, however, that our data does not prove a direct linkage between an enhanced NF-κB signaling and cell growth. It may be possible that CASP8 mutants exert cancer-promoting functions other than the activation of NF-κB pathway.

Importantly, a recent large-scale exome sequencing of HNSCC specimens ($n = 74$) detected somatic mutations of *CASP8* in 8% of tumors,[33] suggestive of an unexpected and transforming role of CASP8 in HNSCC (and maybe also in other epithelial tumors). Whereas activation of NF-κB is frequently detected in a wide array of human malignancies, little is known about the exact mechanisms underlying such activation. Our results show that somatic mutation of *CASP8* may be one such mechanism, and they suggest the possibility of treating *CASP8* mutation-positive tumors with inhibitors of NF-κB, or targeting other proteins that contribute to the NF-κB activation pathway.

Acknowledgments

This study was supported in part by a grant for Research on Human Genome Tailor-made from the Ministry of Health, Labor, and Welfare of Japan, by Grants-in-Aid for Scientific Research (B) from the Japan Society for the Promotion of Science, from The Yasuda Medical Foundation, from The Sagawa Foundation for Promotion of Cancer Research, and from The Mitsubishi Foundation.

Disclosure Statement

The authors have no conflict of interest.

References

1 Mao L, Hong WK, Papadimitrakopoulou VA. Focus on head and neck cancer. *Cancer Cell* 2004; **5**: 311–6.
2 Haddad RI, Shin DM. Recent advances in head and neck cancer. *N Engl J Med* 2008; **359**: 1143–54.
3 Argiris A, Karamouzis MV, Raben D, Ferris RL. Head and neck cancer. *Lancet* 2008; **371**: 1695–709.
4 Mardis ER. A decade's perspective on DNA sequencing technology. *Nature* 2011; **470**: 198–203.
5 Ueno T, Yamashita Y, Soda M *et al.* High-throughput resequencing of target-captured cDNA in cancer cells. *Cancer Sci* 2012; **103**: 131–5.
6 Onishi M, Kinoshita S, Morikawa Y *et al.* Applications of retrovirus-mediated expression cloning. *Exp Hematol* 1996; **24**: 324–9.
7 Langmead B, Trapnell C, Pop M, Salzberg SL. Ultrafast and memory-efficient alignment of short DNA sequences to the human genome. *Genome Biol* 2009; **10**: R25.
8 Hu Q, Milfay D, Williams LT. Binding of NCK to SOS and activation of ras-dependent gene expression. *Mol Cell Biol* 1995; **15**: 1169–74.
9 Takeshita T, Arita T, Higuchi M *et al.* STAM, signal transducing adaptor molecule, is associated with Janus kinase and involved in signaling for cell growth and c-myc induction. *Immunity* 1997; **6**: 449–57.
10 El-Deiry WS, Tokino T, Velculescu VE *et al.* WAF1, a potential mediator of p53 tumor suppression. *Cell* 1993; **75**: 817–25.
11 Kurooka H, Kuroda K, Honjo T. Roles of the ankyrin repeats and C-terminal region of the mouse notch1 intracellular region. *Nucleic Acids Res* 1998; **26**: 5448–55.
12 Hill CS, Wynne J, Treisman R. The Rho family GTPases RhoA, Rac1, and CDC42Hs regulate transcriptional activation by SRF. *Cell* 1995; **81**: 1159–70.
13 Muzio M, Chinnaiyan AM, Kischkel FC *et al.* FLICE, a novel FADD-homologous ICE/CED-3-like protease, is recruited to the CD95 (Fas/APO-1) death–inducing signaling complex. *Cell* 1996; **85**: 817–27.
14 Chaudhary PM, Eby MT, Jasmin A, Kumar A, Liu L, Hood L. Activation of the NF-kappaB pathway by caspase 8 and its homologs. *Oncogene* 2000; **19**: 4451–60.
15 Hu WH, Johnson H, Shu HB. Activation of NF-kappaB by FADD, Casper, and caspase-8. *J Biol Chem* 2000; **275**: 10838–44.
16 Soung YH, Lee JW, Kim SY *et al.* Caspase-8 gene is frequently inactivated by the frameshift somatic mutation 1225_1226delTG in hepatocellular carcinomas. *Oncogene* 2005; **24**: 141–7.
17 Mandruzzato S, Brasseur F, Andry G, Boon T, van der Bruggen P. A CASP-8 mutation recognized by cytolytic T lymphocytes on a human head and neck carcinoma. *J Exp Med* 1997; **186**: 785–93.
18 Kim HS, Lee JW, Soung YH *et al.* Inactivating mutations of caspase-8 gene in colorectal carcinomas. *Gastroenterology* 2003; **125**: 708–15.
19 Soung YH, Lee JW, Kim SY *et al.* CASPASE-8 gene is inactivated by somatic mutations in gastric carcinomas. *Cancer Res* 2005; **65**: 815–21.
20 Eberstadt M, Huang B, Chen Z *et al.* NMR structure and mutagenesis of the FADD (Mort1) death-effector domain. *Nature* 1998; **392**: 941–5.
21 Tibbetts MD, Zheng L, Lenardo MJ. The death effector domain protein family: regulators of cellular homeostasis. *Nat Immunol* 2003; **4**: 404–9.
22 Yu JW, Shi Y. FLIP and the death effector domain family. *Oncogene* 2008; **27**: 6216–27.

© 2013 Japanese Cancer Association

23 Budd RC, Yeh WC, Tschopp J. cFLIP regulation of lymphocyte activation and development. *Nat Rev Immunol* 2006; **6**: 196–204.
24 Kischkel FC, Lawrence DA, Tinel A *et al.* Death receptor recruitment of endogenous caspase-10 and apoptosis initiation in the absence of caspase-8. *J Biol Chem* 2001; **276**: 46639–46.
25 Wang J, Chun HJ, Wong W, Spencer DM, Lenardo MJ. Caspase-10 is an initiator caspase in death receptor signaling. *Proc Natl Acad Sci USA* 2001; **98**: 13884–8.
26 Sprick MR, Rieser E, Stahl H, Grosse-Wilde A, Weigand MA, Walczak H. Caspase-10 is recruited to and activated at the native TRAIL and CD95 death-inducing signalling complexes in a FADD-dependent manner but can not functionally substitute caspase-8. *EMBO J* 2002; **21**: 4520–30.
27 Shikama Y, Yamada M, Miyashita T. Caspase-8 and caspase-10 activate NF-kappaB through RIP, NIK and IKKalpha kinases. *Eur J Immunol* 2003; **33**: 1998–2006.
28 Pop C, Fitzgerald P, Green DR, Salvesen GS. Role of proteolysis in caspase-8 activation and stabilization. *Biochemistry* 2007; **46**: 4398–407.
29 Krammer PH. CD95's deadly mission in the immune system. *Nature* 2000; **407**: 789–95.
30 Heyninck K, Beyaert R. Crosstalk between NF-kappaB-activating and apoptosis-inducing proteins of the TNF-receptor complex. *Mol Cell Biol Res Commun* 2001; **4**: 259–65.
31 Varfolomeev E, Maecker H, Sharp D *et al.* Molecular determinants of kinase pathway activation by Apo2 ligand/tumor necrosis factor-related apoptosis-inducing ligand. *J Biol Chem* 2005; **280**: 40599–608.
32 Golks A, Brenner D, Krammer PH, Lavrik IN. The c-FLIP-NH2 terminus (p22-FLIP) induces NF-kappaB activation. *J Exp Med* 2006; **203**: 1295–305.
33 Stransky N, Egloff AM, Tward AD *et al.* The mutational landscape of head and neck squamous cell carcinoma. *Science* 2011; **333**: 1157–60.

Supporting Information

Additional Supporting Information may be found in the online version of this article:

Fig. S1. Non-synonymous mutations in caspase-8. CRC, colorectal cancer; GC, gastric cancer; HCC, hepatocellular carcinoma; HNSCC, head and neck squamous cell carcinoma.

Fig. S2. Caspase-8 (CASP8) affects annexin V-positive fractions in T3M-1 Cl-10 head and neck squamous cell carcinoma cells but not in OE21 esophageal squamous cell carcinoma cells.

Fig. S3. Depletion of *CASP8* message leads to a decrease in *BCL2* expression.

Fig. S4. Structure of human death effector domain (DED) family members.

Table S1. Caspase-8 (CASP8) non-synonymous mutations identified in previously published reports.

doi: 10.1111/cas.12191
© 2013 Japanese Cancer Association

Miyanaga et al. BMC Cancer 2013, 13:262
http://www.biomedcentral.com/1471-2407/13/262

BMC Cancer

CASE REPORT Open Access

Activity of EGFR-tyrosine kinase and ALK inhibitors for *EML4–ALK*-rearranged non–small–cell lung cancer harbored coexisting *EGFR* mutation

Akihiko Miyanaga[1], Kumi Shimizu[1], Rintaro Noro[1], Masahiro Seike[1], Kazuhiro Kitamura[1], Seiji Kosaihira[1], Yuji Minegishi[1], Takehito Shukuya[7], Akinobu Yoshimura[1,8], Masashi Kawamoto[2,3], Shinichi Tsuchiya[2], Koichi Hagiwara[4], Manabu Soda[5], Kengo Takeuchi[6], Nobuyuki Yamamoto[7], Hiroyuki Mano[5], Yuichi Ishikawa[6] and Akihiko Gemma[1*]

Abstract

Background: The *EML4–ALK* (echinoderm microtubule-associated protein-like 4 gene and the anaplastic lymphoma kinase gene) fusion oncogene represents a novel molecular target in a small subset of non–small–cell lung cancers (NSCLCs). The *EML4–ALK* fusion gene occurs generally in NSCLC without mutations in epidermal growth factor receptor *(EGFR)* and *KRAS*.

Case presentation: We report that a case of *EML4–ALK*-positive NSCLC with *EGFR* mutation had a response of stable disease to both an EGFR tyrosine kinase inhibitor (EGFR-TKI) and ALK inhibitor.

Conclusions: We described the first clinical report of a patient with *EML4–ALK*-positive NSCLC with *EGFR* mutation that had a response of stable disease to both single-agent EGFR-TKI and ALK inhibitor. *EML4–ALK* translocation may be associated with resistance to EGFR-TKI, and EGFR signaling may contribute to resistance to ALK inhibitor in *EML4–ALK*-positive NSCLC.

Keywords: EML4–ALK, *EGFR* mutation, Lung cancer

Background

The *EML4–ALK* (echinoderm microtubule-associated protein-like 4 gene and the anaplastic lymphoma kinase gene) fusion oncogene was recently identified as a novel genetic alteration in non-small-cell lung cancer (NSCLC) [1]. *EML4–ALK* fusions have been detected in 2 to 7% of NSCLC patients. Patients harboring *ALK* rearrangements tend to be never and light smokers, have a history of adenocarcinoma, and be younger in age [1-6]. In general, the *EML4–ALK* fusion oncogene existed exclusively in NSCLC patients without the epidermal growth factor receptor (*EGFR*) gene mutation [1,7,8].

ALK inhibitors such as crizotinib are clinically effective in NSCLC patients harboring ALK rearrangements [9]. Crizotinib produced a high response rate and prolonged median progression-free survival among patients with ALK-positive NSCLC [9]. Crizotinib was recently approved by the US Food and Drug Administration and Japanese Ministry of Health, Labour and Welfare for the treatment of patients with advanced, ALK-rearranged NSCLC.

In this paper, we report a patient with NSCLC with concomitant ALK rearrangement and *EGFR* mutation that had a response of stable disease to both an EGFR tyrosine kinase inhibitor (EGFR-TKI) and ALK inhibitor.

Case presentation

In December 2009, a 55-year-old female who had never smoked was noted to have left lung opacity on a routine chest X-ray. No significant previous medical history was reported. Computed tomography (CT) scan of the chest revealed a 1.5 × 1.5 cm nodular lesion in the left upper lobe and hilar lymph node metastasis. Transthoracic needle biopsy histology revealed adenocarcinoma, and the histopathological subtype of the specimen was

* Correspondence: agemma@nms.ac.jp
[1]Department of Pulmonary Medicine and Oncology, Graduate School of Medicine, Nippon Medical School, Tokyo, Japan
Full list of author information is available at the end of the article

BioMed Central

© 2013 Miyanaga et al.; licensee BioMed Central Ltd. This is an Open Access article distributed under the terms of the Creative Commons Attribution License (http://creativecommons.org/licenses/by/2.0), which permits unrestricted use, distribution, and reproduction in any medium, provided the original work is properly cited.

papillary adenocarcinoma with signet-ring cell components (Figure 1A-1C). The specimen was positive for periodic acid–Schiff (PAS) (Figure 1C). On immunohistochemical staining, the tumor cells were positive for thyroid transcription factor-1 (TTF-1) (Figure 1D). Laboratory findings were within normal range, except for the carcinoembryonic antigen (CEA) level of 158.0 ng/mL (normal range, 0 to 4.3 ng/mL) in the serum. She had multiple dorsal vertebra metastases (cT1N1M1b, stage IV).

Analysis for *EGFR* gene mutation was performed using a cytological specimen by means of the peptide nucleic acid–locked nucleic acid (PNA-LNA) polymerase-chain-reaction (PCR) clamp method as described previously [10,11]. The specimen showed a deletion in exon 19 (L747-A750del T751S). We collected mRNA from the same tumor specimens using Pinpoint Slide RNA Isolation System in order to clarify whether there was *EML4–ALK* (echinoderm microtubule-associated protein-like 4 gene and the anaplastic lymphoma kinase gene) fusion gene in each tumor. Reverse transcription polymerase-chain-reaction (RT-PCR) followed by direct sequencing confirmed the presence of *EML4–ALK* variant 2 [1] (Figure 2). In addition, *EML4–ALK* was identified by using fluorescent in situ hybridization (FISH) for *ALK* rearrangements (Figure 3B) and was confirmed by immunohistochemistry for ALK expression in tumor [2] (Figure 3A).

A platinum doublet was chosen as first line therapy according to existing treatment protocol in 2009. Four cycles of combination chemotherapy comprising cisplatin and pemetrexed was administered at 3-week intervals. She was judged as having a stable disease. After 7 months, spinal magnetic resonance imaging (MRI) revealed progression of the dorsal vertebra lesions. Therefore, EGFR-TKI was chosen as a 2nd-line therapy. She received gefitinib therapy at 250 mg/day administered orally for 2 months. CT imaging of the chest showed that the pulmonary nodule was not growing after gefitinib therapy, and the tumor marker levels had not changed. However, spinal MRI demonstrated growing dorsal vertebra metastases 2 months after the start of gefitinib therapy. The carcinoembryonic antigen (CEA) level increased from 117 ng/ml to 250 ng/ml. Therefore, the patient was judged as having progressive disease. After local radiation therapy with a total of 30 Gy for dorsal metastases, a second EGFR-TKI was chosen given the stable primary disease. She received another EGFR-TKI, erlotinib (150 mg/day), as 3rd-line therapy. After being progression-free for 3 months, spinal MRI revealed a growing thoracic vertebra metastasis. She received 4th-line treatment with 2 cycles of docetaxel (DTX). However, her disease progressed 6 months later. Finally, she received a targeted inhibitor of ALK. The patient initially had SD associated with a temporary decrease in the CEA level from 743 ng/ml to 520 ng/ml, but her disease progressed after 4 months of therapy. The ALK inhibitor treatment was

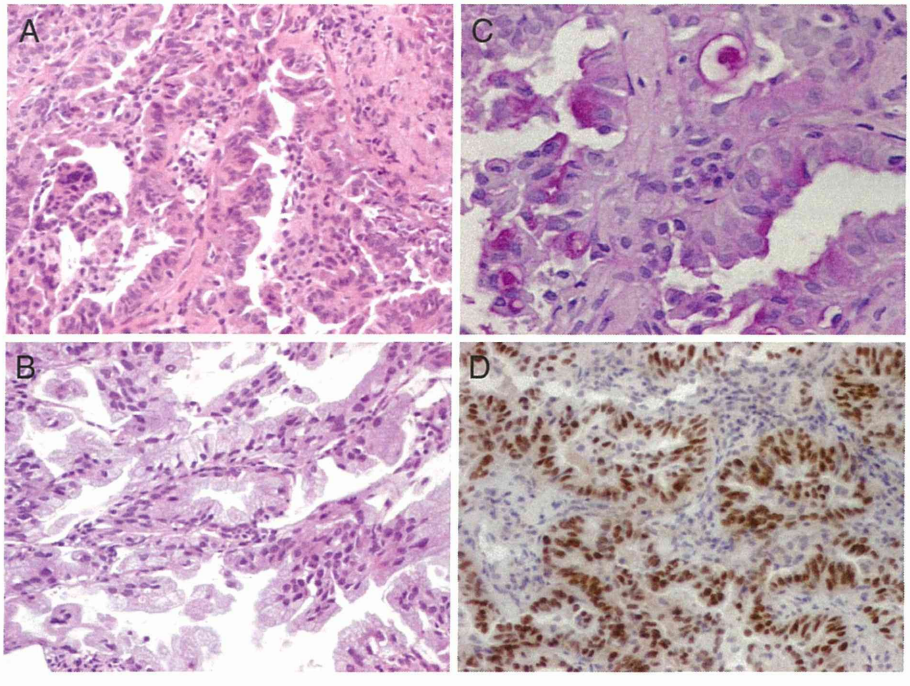

Figure 1 Histology of the primary tumour. (**A**) and (**B**) shows a papillary adenocarcinoma (hematoxylin and eosin 200× magnification), (**C**) a mucin stain shows positive for both signet-ring and papillary morphology (PAS, 400× magnification). **(D)** immunohistochemical analysis of lung adenocarcinoma specimens with *EML4-ALK* fusion using a monoclonal anti-TTF-1 antibody (200× magnification).